



## FABRICATION AND TEST OF A FLUERIC POSITION SERVO

Prepared for  
NATIONAL AERONAUTICS AND SPACE ADMINISTRATION

CONTRACT NAS 3-6201

|                   |                               |            |
|-------------------|-------------------------------|------------|
| FACILITY FORM 502 | N67 14925                     |            |
|                   | (ACCESSION NUMBER)            | (THRU)     |
|                   | 31                            | 1          |
|                   | (PAGES)                       | (CODE)     |
|                   | CR-72129                      | 03         |
|                   | (NASA CR OR TMX OR AD NUMBER) | (CATEGORY) |


By

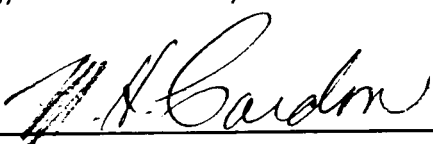
THE BENDIX CORPORATION  
RESEARCH LABORATORIES DIVISION  
Southfield, Michigan

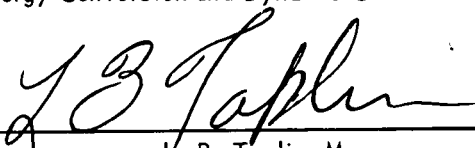
GPO PRICE \$ \_\_\_\_\_  
CFSTI PRICE(S) \$ \_\_\_\_\_  
Hard copy (HC) 3.00  
Microfiche (MF) 65

# Progress Report

## FABRICATION AND TEST OF A FLUERIC POSITION SERVO

Prepared by:   
L. R. Erwin, Senior Engineer  
Machine and Propulsion Controls Department  
Energy Conversion and Dynamic Controls Laboratory

Approved by:   
M. H. Cardon, Project Engineer  
Machine and Propulsion Controls Department  
Energy Conversion and Dynamic Controls Laboratory

Approved by:   
L. B. Taplin, Manager  
Energy Conversion and Dynamic Controls Laboratory

Prepared for  
NATIONAL AERONAUTICS AND SPACE ADMINISTRATION

10 December 1965 to 10 June 1966

CONTRACT NAS 3-6201

Technical Management  
NASA Lewis Research Center  
Cleveland, Ohio 44135  
Advanced Systems Division  
Vernon D. Gebben

By

The Bendix Corporation  
Research Laboratories Division  
Southfield, Michigan 48075

## TABLE OF CONTENTS

|   | <u>Page</u> |
|---|-------------|
| SECTION 1 - INTRODUCTION  | 1-1         |
| SECTION 2 - SUMMARY   | 2-1         |
| SECTION 3 - MECHANICAL DESIGN   | 3-1         |
| SECTION 4 - BREADBOARD FLUERIC CIRCUIT  | 4-1         |
| 4.1 Lead-Lag Circuit  | 4-1         |
| 4.2 Flueric Circuit Components  | 4-4         |
| 4.3 Single-Input Vortex Amplifier Development                                     | 4-6         |
| SECTION 5 - GOALS OF THE FOURTH QUARTER   | 5-1         |
| APPENDIX A - VARIATION OF FREQUENCY RESPONSE<br>WITH GAS CONSTANT AND TEMPERATURE | A-1         |

## LIST OF ILLUSTRATIONS

| <u>Figure No.</u> | <u>Title</u>   | <u>Page</u> |
|-------------------|--|-------------|
| 3-1               | Power Control Valve Test Fixture and<br>Control Circuit Adaptors                                   | 3-2         |
| 3-2               | Component Parts of Error Detector  | 3-2         |
| 3-3               | Component Parts of Power Control Valve   | 3-2         |
| 4-1               | Schematic Diagram of the Lead-Lag Circuit  | 4-2         |
| 4-2               | Initial Breadboard Lead-Lag Circuit  | 4-3         |
| 4-3               | Closed-Loop Frequency Response of<br>Breadboard Lead-Lag Circuit                                   | 4-3         |
| 4-4               | Schematic Diagram of the Lead-Lag Circuit<br>Showing Diffusion-Bonded Packages                     | 4-5         |
| 4-5               | Second Breadboard Lead-Lag Circuit   | 4-5         |
| 4-6               | No-Load Gain Characteristics of an<br>Unbonded SIVA-36   | 4-6         |
| 4-7               | No-Load Gain Characteristics of a Bonded<br>SIVA-36  | 4-7         |
| 4-8               | No-Load Gain Characteristics of Two<br>SIVA-36 Operating as a Push-Pull Pair                       | 4-7         |
| 4-9               | No-Load Gain Characteristics of the Single-<br>Input Vortex Amplifier with a Stabilizing<br>Baffle | 4-8         |
| 4-10              | SIVA-36 and Variations   | 4-10        |
| 4-11              | SIVA-37 and 38 and Variations  | 4-12        |
| A-1               | Compressible Flow Through a Tank   | A-2         |

| <u>Table No.</u> | <u>Title</u>                               | <u>Page</u> |
|------------------|--|-------------|
| 4-1              | Summary of Results of SIVA Stability Tests | 4-11        |

FABRICATION AND TEST  
OF A FLUERIC POSITION SERVO

Prepared by: L. R. Erwin

Approved by: M. H. Cardon and L. B. Taplin

ABSTRACT

This report is the third quarterly report of Task 2 of a program to develop a pneumatic control drum actuator for a nuclear rocket engine in which the electronics have been replaced by flueric devices. The objective of the Task 2 effort is to fabricate and test the system designed and studied in Task 1.

In this quarter, the detailed drawings for the Position Error Detector Unit and Power Control Valve were released. Many purchased items have been received and a number of machined parts have been completed. Improvements were made on the flueric vortex pressure amplifiers. A breadboard lead-lag circuit was built and tested.

## SECTION 1

### INTRODUCTION

This report is the third quarterly report of Task 2 of a two-task effort to develop a pneumatic actuation system in which the electronics that formerly provided the error detection, frequency compensation, and amplification have been replaced with flueric devices.

In Task 1, an all-pneumatic servo actuator with performance characteristics comparable to an existing electropneumatic system was designed and analytically studied. The existing electropneumatic actuation system selected for a base in the study is used to position control drums in a nuclear rocket engine. The results of Task 1 are presented in a Summary Report,\* dated August 31, 1965. The objective of Task 2 of the effort is to fabricate the system designed in Task 1 and to evaluate it experimentally.

In this report, progress toward the completion of the Position Error Detector Unit and Power Control Valve are discussed. Test results of a breadboard lead-lag circuit are presented. Single-input vortex amplifier design improvements are discussed.

---

\* "Replacement of Electronics With Fluid Interaction Devices" (Task 1, Summary Report), NASA CR-54758, (N65-34912), August 31, 1965. Requests for copies should be referred to the Federal Scientific and Technical Information Office, Port Royal Road, Springfield, Virginia, 22151. Identification No. N65-34912, Category CSCL 13G. Two dollars for full-size copy; fifty cents for microfilm copy.

## SECTION 2

### SUMMARY

In this quarter, the detail drawings of the Position Error Detector Unit and Power Control Valve were completed and released for manufacture. Many purchased items have been received, and a number of machined parts have been completed.

A breadboard lead-lag circuit was assembled and tested. The frequency response demonstrated the desired lead-lag characteristics. A second, more compact, lead-lag circuit has been constructed to minimize component lags.

Vortex components have been successfully fabricated in push-pull pairs.

An instability that existed in earlier single-input vortex amplifiers has been eliminated.

### SECTION 3

#### MECHANICAL DESIGN

All detail drawings on both the Position Error Detector Unit and the Power Control Valve have been completed and released for manufacture. Completion of the parts for these components is scheduled for mid-July. All purchased parts have been received except the metallic seals for both the Power Control Valve and Error Detector Unit. Initial tests of these devices will be conducted with rubber seals used in place of the metallic seals.

Actuator test fixture parts have been designed and released for manufacture. The parts are scheduled for completion by the end of July. Figures 3-1 through 3-3 show some of the parts which have been completed for the various mechanical components.



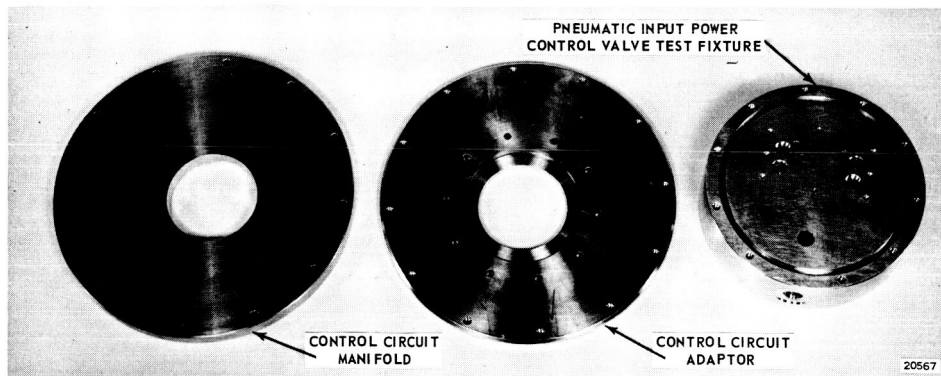


Figure 3-1 - Power Control Valve Test Fixture and Control Circuit Adaptors

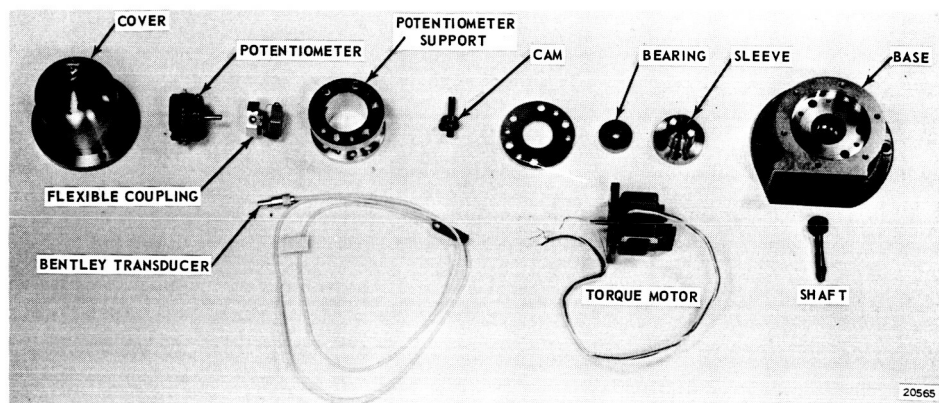


Figure 3-2 - Component Parts of Error Detector

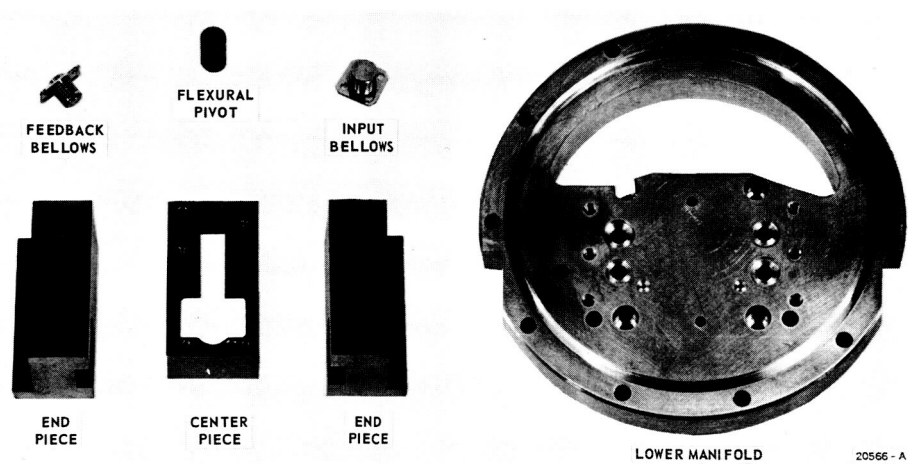


Figure 3-3 - Component Parts of Power Control Valve

## SECTION 4

### BREADBOARD FLUERIC CIRCUIT

The design goal for flueric circuit work for this quarter was to complete breadboard tests on the flueric circuit.

Tests of the initial breadboard lead-lag circuit were completed and the circuit demonstrated the desired characteristics. A second, more compact, lead-lag circuit has been constructed and will be tested presently. A stability problem that developed in the single-input vortex amplifier has been corrected.

#### 4.1 LEAD-LAG CIRCUIT

The initial breadboard lead-lag circuit consisted of individual breadboard vortex elements connected by nylon tubing. The vortex elements were not bonded at this point; instead, the laminated plates were clamped securely to the test blocks. Figure 4-1 shows the circuit schematic, and Figure 4-2 shows the breadboarded circuit, with elements spread apart and connected by long lines for convenience in making the adjustments required in the early stages of development.

The tests conducted on the initial breadboard circuit determined its frequency response, static performance, and circuit noise. The results of the frequency response test, plotted in Figure 4-3, show that the desired lead-lag characteristics were achieved.

The break points, of course, are not at the specified frequencies because of the long flexible tubing and large volumes of the breadboard circuit. Since it is not compact, the breadboard circuit has relatively large stage lags that occur at a lower frequency than is specified for the final configuration. To exhibit the desired lead-lag form, it was necessary for the lead characteristic to occur at a still lower frequency so that the lead-lag characteristics would not be obscured by the large stage lags; therefore, the tanks in the feedback circuits that generate the lead term were made larger than the design value.

Having demonstrated that this circuit produces the desired lead-lag characteristics, it is now possible to shift the break points to a higher frequency by changing circuit volume, gas constant and gas

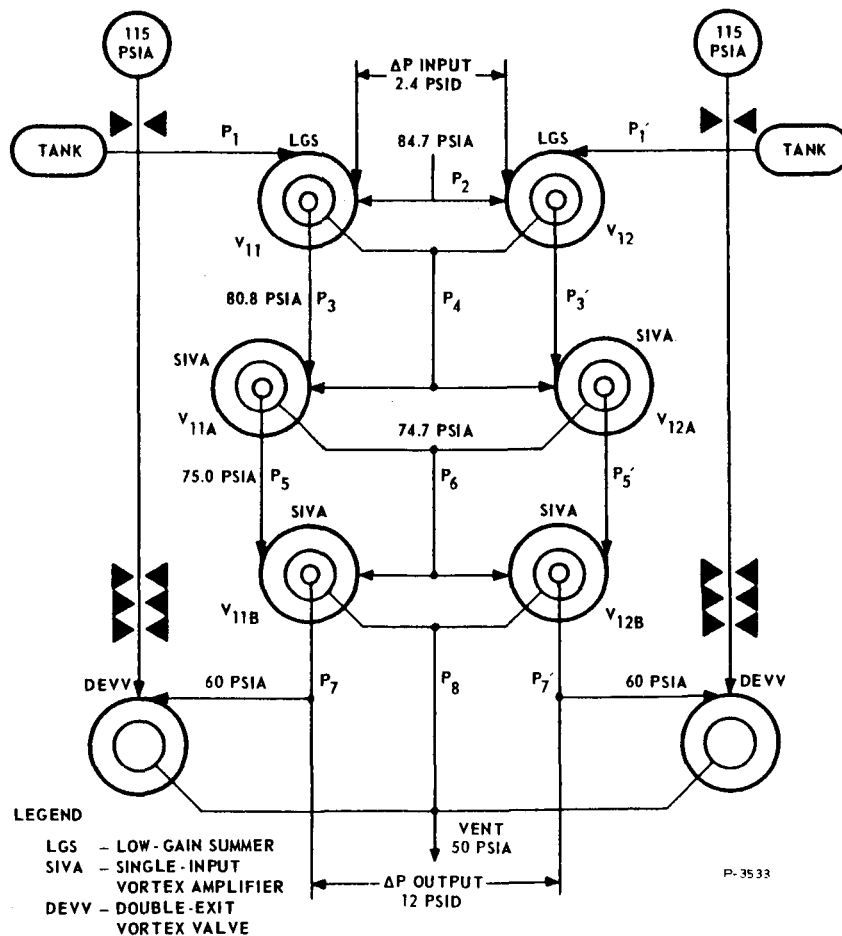


Figure 4-1 - Schematic Diagram of the Lead-Lag Circuit

temperature. For example, repackaging the circuit to reduce all volumes by a factor of three will increase the frequency scale by the same factor. Using 600°R hydrogen rather than 530°R nitrogen will increase the frequency scale by a factor of four. Appendix A demonstrates the method of frequency response scaling with gas constant and temperature. Repackaging and using 600°R hydrogen would increase the frequency response to the specified range.

An apparent instability occurred when the circuit was in the balanced condition. This was later traced to the single-input vortex amplifier design. The amplifier design was revised, and tests of a push-pull pair indicate that the instability has been corrected. This development is discussed thoroughly in Section 4.3. It is difficult to distinguish

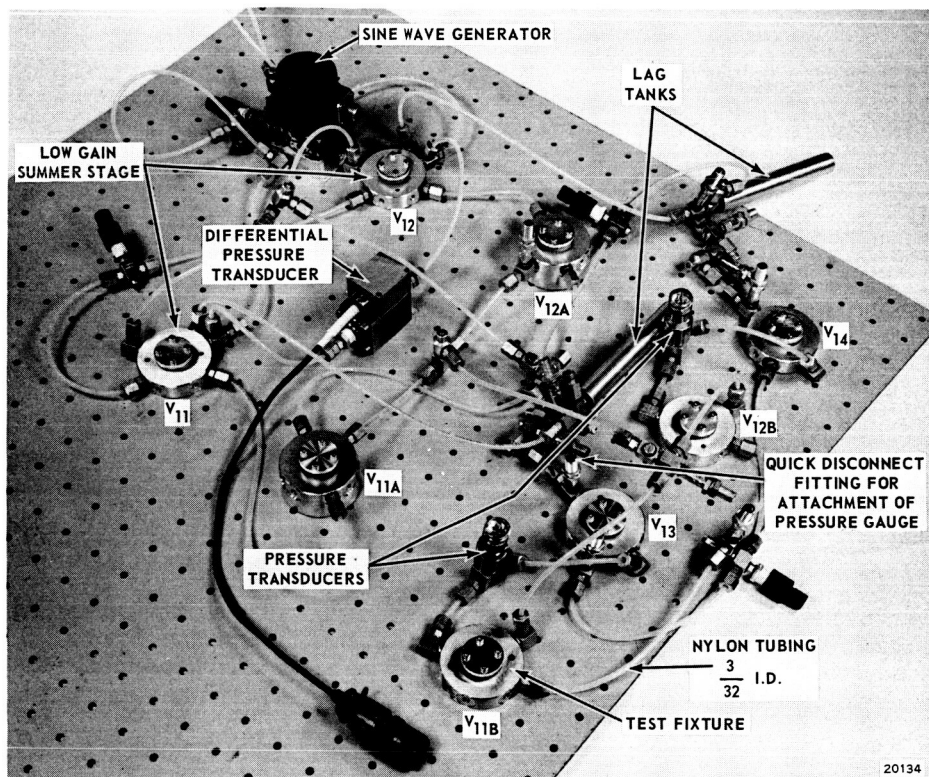


Figure 4-2 - Initial Breadboard Lead-Lag Circuit

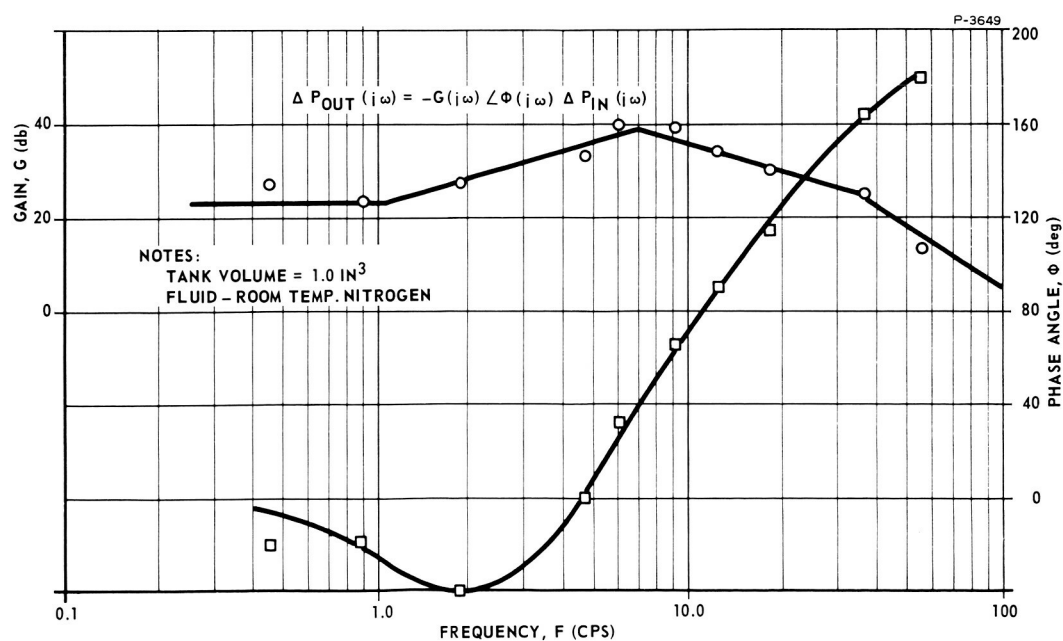


Figure 4-3 - Closed-Loop Frequency Response of Breadboard Lead-Lag Circuit

between the instability and circuit noise, but the circuit noise appeared to be about  $\pm 0.7$  psi.

In static performance tests, the required  $\pm 12$  psid output stage swing was achieved by adding a small amount of supply flow to the output push-pull stage. This was done as a convenience in the initial breadboard circuit; in the final design, pressure levels at previous stages will be adjusted to achieve the same result. The circuit operated with a balanced output only when the input was unbalanced with about 1.0 psid. Some of this unbalance is in the forward path, but most of it appears to be in the feedback path. It is felt that, when component leakages are eliminated, and the adjustable orifices in the feedback circuit, which are extremely sensitive, are replaced with fixed orifices, the unbalance will be reduced substantially.

The schematic diagram of the second breadboard lead-lag circuit is shown in Figure 4-4. This is functionally the same diagram as that of Figure 4-1. The only difference is that Figure 4-4 shows the manner in which the circuit components are combined. Figure 4-5 is a photograph of the second breadboard lead-lag circuit. A comparison with Figure 4-2 shows that the second breadboard circuit is considerably more compact. The amplifiers were all bonded to eliminate leakage. Each individual amplifier was bonded and tested, and then the amplifiers were bonded in push-pull pairs. Each stack contains a push-pull stage and the required ducting and orifices. Quick-connects are used to attach pressure gauges at intermediate points. Copper tubing is used to shorten the lines between stages. This circuit is still larger than the final configuration, but this configuration will verify the scaling of frequency response with circuit dimensions. The frequency response of this circuit will be obtained shortly.

Breadboarding of the position error circuit and the summing stage has been started.

#### 4.2 FLUERIC CIRCUIT COMPONENTS

The flueric circuit components have been successfully fabricated in push-pull pairs, eliminating all leaks that were present with the clamped components. The components have been fabricated in their final design. Thus, after component tests are successfully completed, these components can be incorporated in the final system.

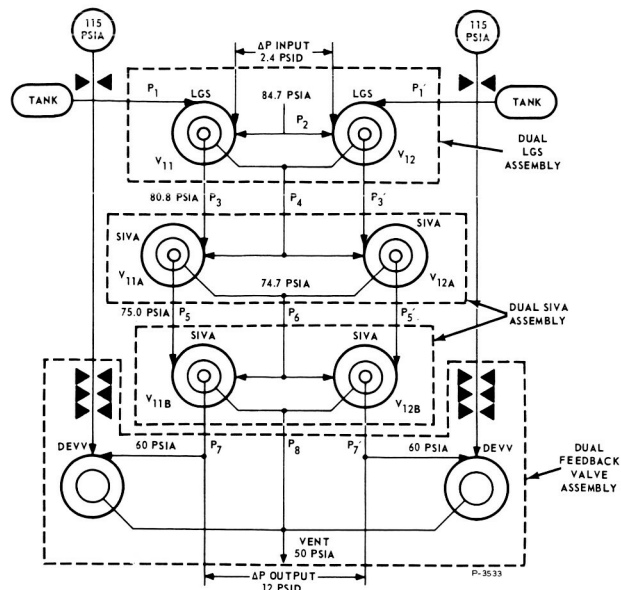


Figure 4-4 - Schematic Diagram of the Lead-Lag Circuit Showing Diffusion-Bonded Packages

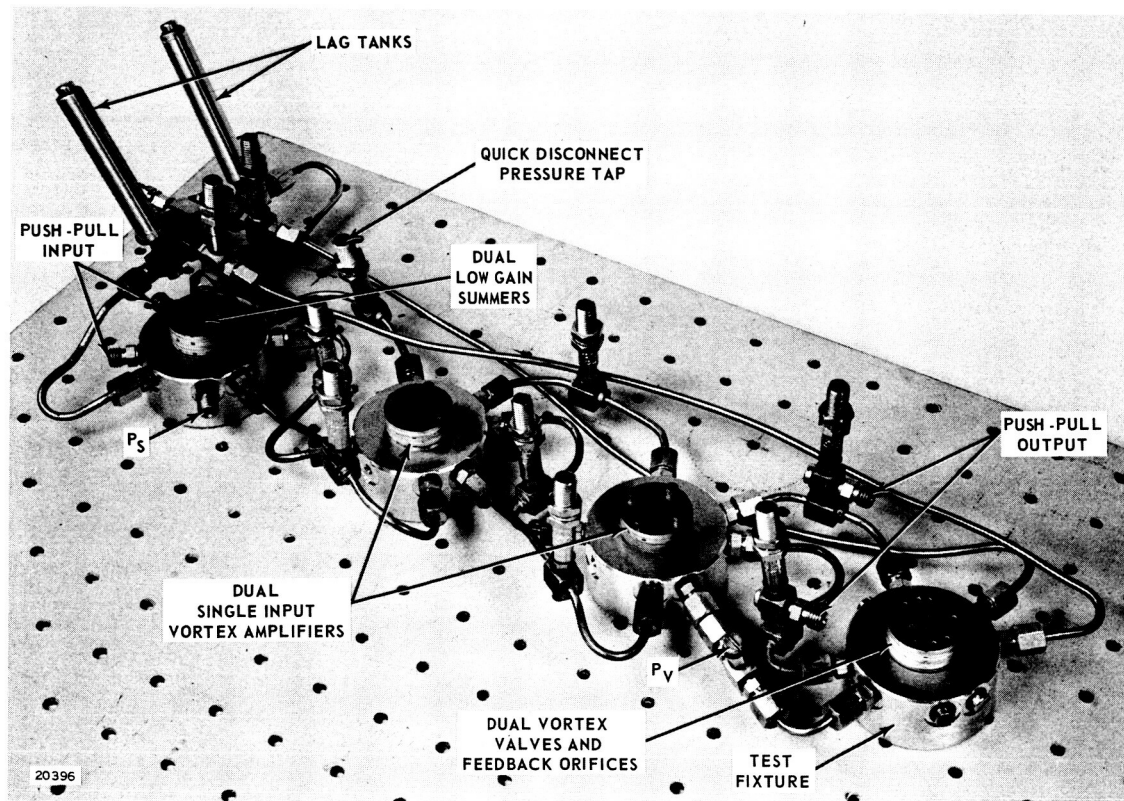


Figure 4-5 - Second Breadboard Lead-Lag Circuit

### 4.3 SINGLE-INPUT VORTEX AMPLIFIER DEVELOPMENT

The single-input vortex amplifier used in the initial breadboard lead-lag circuit of Figure 4-2 (SIVA-36) had a small region of instability as output pressure ( $P_o$ ) approached vent pressure ( $P_v$ ). This instability appears as vertical sections on the no-load pressure gain characteristics of Figure 4-6. It was believed that this region could be avoided except during transients and thus would not cause trouble. This was not the case and the lead-lag circuit had an instability at the balanced condition. After diffusion bonding, the chamber losses had been reduced and the pressure gain characteristics were as shown in Figure 4-7. When the high-gain bonded amplifiers were arranged in a push-pull pair, the differential input and output were as shown in Figure 4-8. The differential input was driven by a servovalve using a triangular wave input. The output pressure jumped as the amplifiers were driven through the unstable region. Because of the low pressure drop across the injector nozzles, the jump was reflected back to the input.

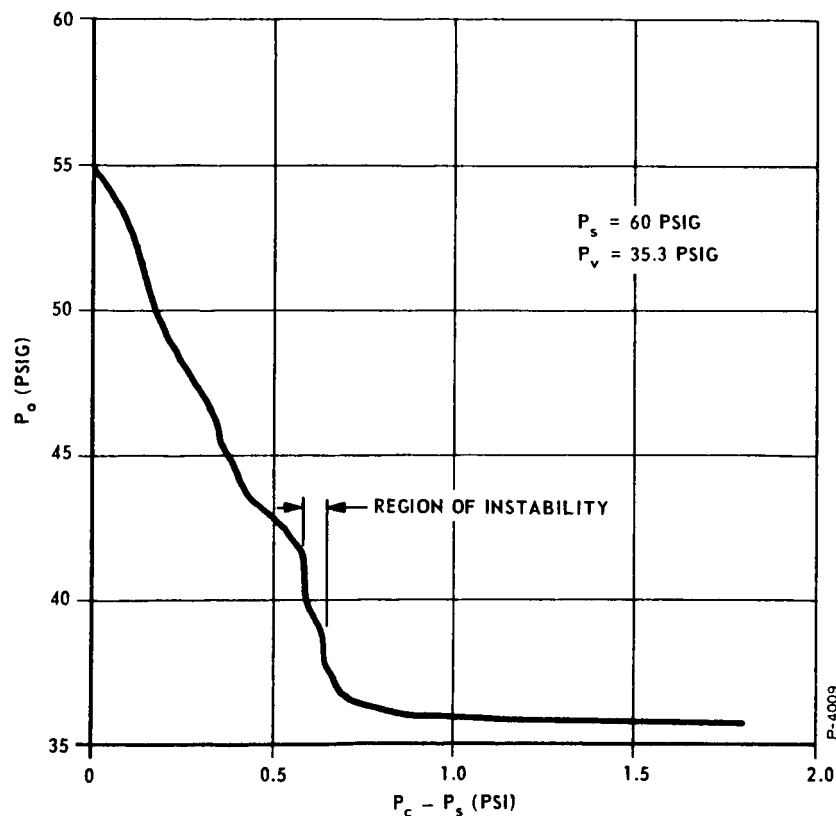


Figure 4-6 - No-Load Gain Characteristics of an Unbonded SIVA-36

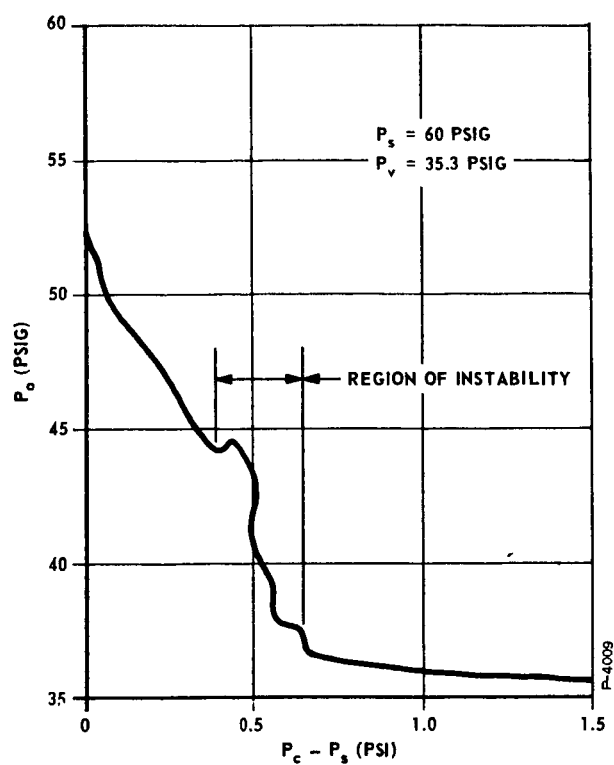


Figure 4-7 - No-Load Gain Characteristics of a Bonded SIVA-36

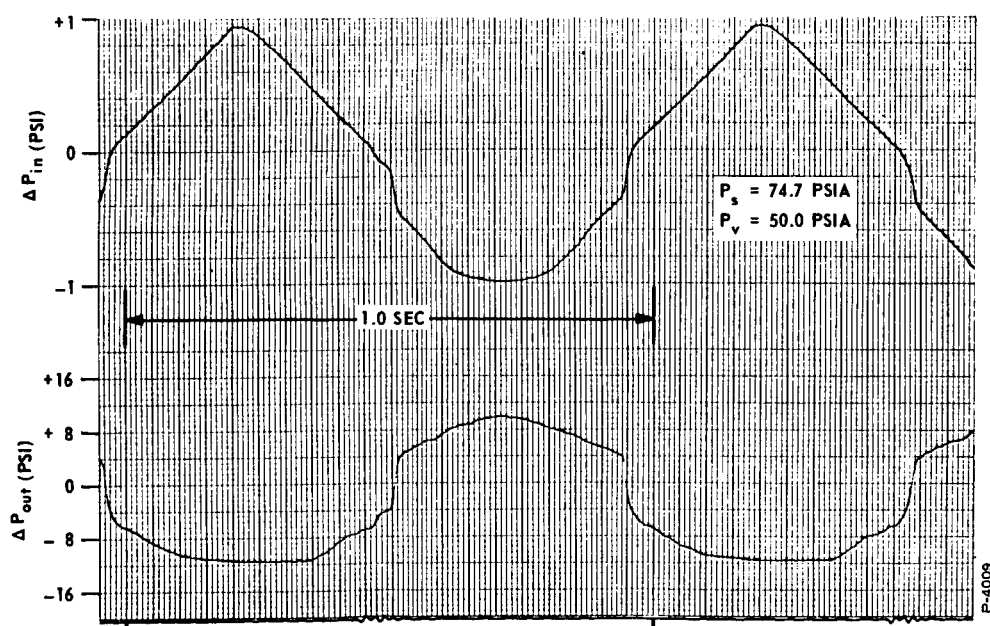


Figure 4-8 - No-Load Gain Characteristics of Two SIVA-36 Operating as a Push-Pull Pair



Several vortex chamber redesigns were tested in an attempt to eliminate the instability without adversely affecting the gain or maximum pressure swing. In the vortex chamber redesigns, variations were made in the vortex chamber length; size, position and number of tangential control orifices; and the button configuration. Also, vortex chambers with various types of baffles in the end of the chamber and the use of auxiliary supply flows were investigated. The instability was eliminated by the introduction of a baffle in the end of the vortex chamber that increased vortex chamber losses. No changes were made in the already established vortex chamber and button size, receiver size and configuration, vortex chamber outlet size and configuration, or the distance between the outlet orifice and receiver.

Tests were conducted on single amplifiers and pairs operating in push-pull. In these tests, the input control signal was varied through its operating range, using a flapper nozzle valve driven by a torque motor. The input control signal and output pressure were measured and recorded by a two-channel strip chart recorder. From the strip charts, instability could be seen and the amplifier gain was determined.

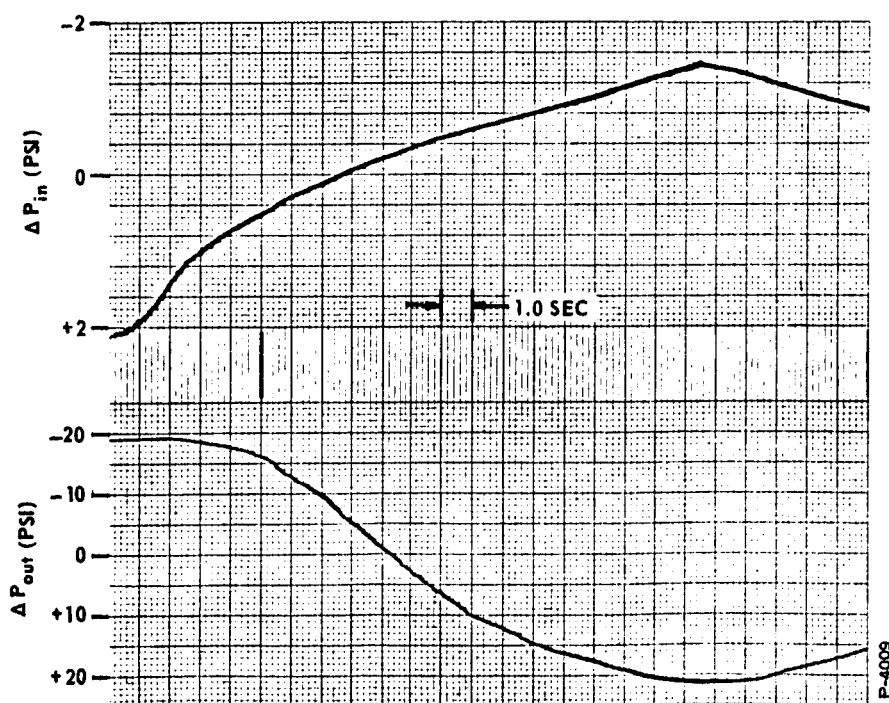
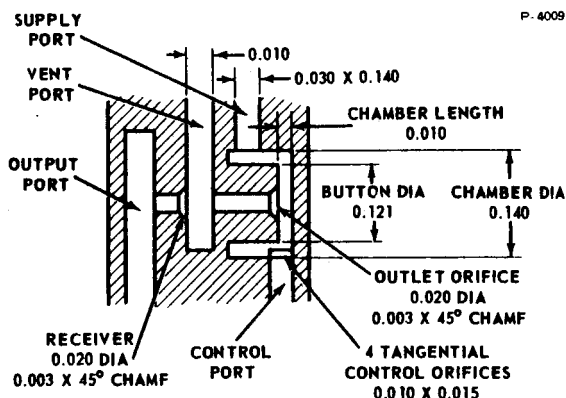
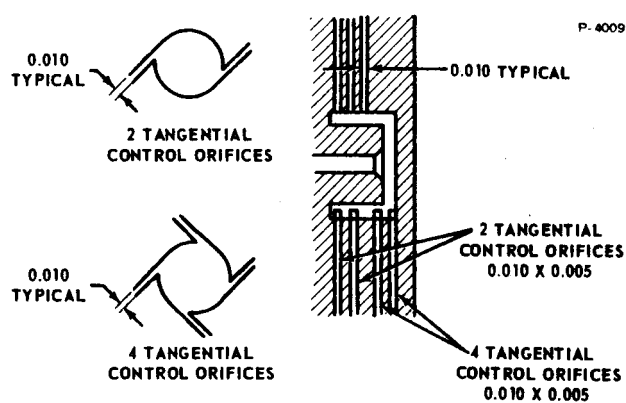


Figure 4-9 - No-Load Gain Characteristics of the Single-Input Vortex Amplifier with a Stabilizing Baffle

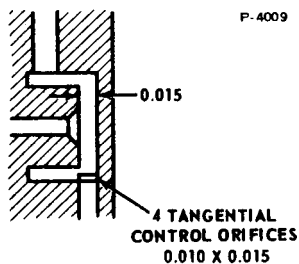
Redesigns were made and tested until a design was achieved that exhibited the stable performance shown in Figure 4-9. The results of these tests are summarized in Table 4-1. In Figures 4-10 and 4-11, the changes made in redesigns are illustrated and pertinent dimensions are indicated. Stability while maintaining relatively high gain was achieved by the addition of a baffle plate in the end of the vortex chamber. The configuration of this amplifier and pertinent dimensions are shown in Figure 4-11(1), and its no-load gain characteristics are shown in Figure 4-9.



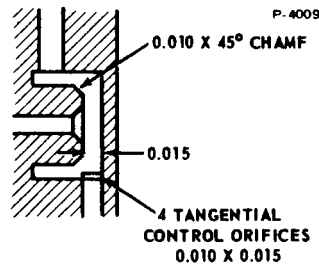
(a) Original SIVA 36



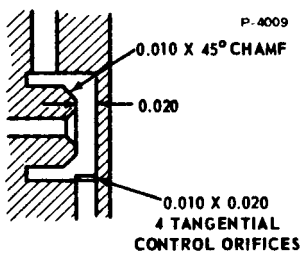
(b) Multi-Control Orifices



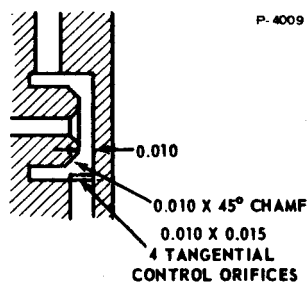
(c) Increased Chamber Length



(d) Increased Chamber Length and Chamfered Button



(e) Increased Chamber Length and Control Orifice Area



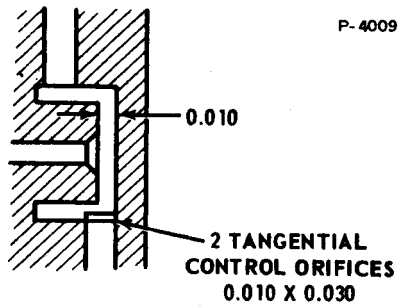
(f) Original Configuration With Chamfered Button

Figure 4-10 - SIVA-36 and Variations

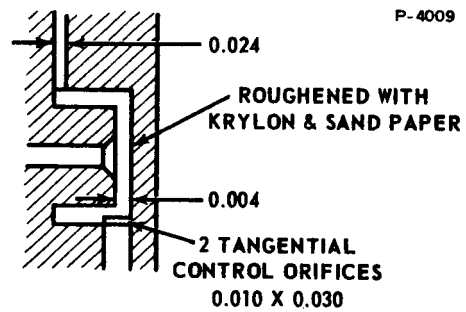
Table 4-1 - Summary of Results of SIVA Stability Tests

| Amplifier Design Figure No.          | Supply Port Size Inch | Port Area In <sup>2</sup> | Tangential Control No. | Control Size Inch | Orifices Area In <sup>2</sup> | Chamber Length Inch | Average Gain psi/psi | Stability                   | Remarks  |
|--------------------------------------|-----------------------|---------------------------|------------------------|-------------------|-------------------------------|---------------------|----------------------|-----------------------------|--|
| SIVA 36 and Variation Figure 4-10(a) | 0.030 x 0.140         | 4.2 x 10 <sup>-3</sup>    | 4                      | 0.010 x 0.015     | 0.6 x 10 <sup>-3</sup>        | 0.010               | 22                   | Unstable                    |  |
| Figure 4-10(b)                       | (3)0.010 x 0.140      | 4.2 x 10 <sup>-3</sup>    |                        | See Figure        | 0.6 x 10 <sup>-3</sup>        | 0.011               | 10.4                 | Improved But Still Unstable |  |
| Figure 4-10(c)                       | 0.030 x 0.140         | 4.2 x 10 <sup>-3</sup>    | 4                      | 0.010 x 0.015     | 0.6 x 10 <sup>-3</sup>        | 0.015               | Not Determined       | Unstable                    |  |
| Figure 4-10(d)                       | 0.030 x 0.140         | 4.2 x 10 <sup>-3</sup>    | 4                      | 0.010 x 0.015     | 0.6 x 10 <sup>-3</sup>        | 0.015               | 13.65                | Improved                    | 0.010 Chamfer On Button                            |
| Figure 4-10(e)                       | 0.030 x 0.140         | 4.2 x 10 <sup>-3</sup>    | 4                      | 0.010 x 0.020     | 0.8 x 10 <sup>-3</sup>        | 0.020               | 9.4                  | Good                        | 0.010 Chamfer On Button                            |
| Figure 4-10(f)                       | 0.030 x 0.140         | 4.2 x 10 <sup>-3</sup>    | 4                      | 0.010 x 0.015     | 0.6 x 10 <sup>-3</sup>        | 0.010               | 10.7                 | Improved                    | Same as 4-10a Except for 0.010 Chamfer On Button   |
| SIVA 37 and Variation Figure 4-11(a) | 0.030 x 0.140         | 4.2 x 10 <sup>-3</sup>    | 2                      | 0.010 x 0.030     | 0.6 x 10 <sup>-3</sup>        | 0.010               | 26.2                 | Unstable                    |  |
| Figure 4-11(b)                       | 0.024 x 0.140         | 3.36 x 10 <sup>-3</sup>   | 2                      | 0.010 x 0.030     | 0.6 x 10 <sup>-3</sup>        | 0.004               | Not Determined       | Good                        | Chamber End Roughened with Krylon and Sandpaper    |
| Figure 4-11(c)                       | 0.030 x 0.140         | 4.2 x 10 <sup>-3</sup>    | 2                      | 0.010 x 0.030     | 0.6 x 10 <sup>-3</sup>        | 0.015               | Not Determined       | Unstable                    | See Auxiliary Supply in Figure                     |
| Figure 4-11(d)                       | 0.030 x 0.140         | 4.2 x 10 <sup>-3</sup>    | 2                      | 0.010 x 0.025     | 0.5 x 10 <sup>-3</sup>        | 0.010               | Not Determined       | Unstable                    | See Auxiliary Supply in Figure                     |
| Figure 4-11(e)                       | 0.030 x 0.140         | 4.2 x 10 <sup>-3</sup>    | 4                      | 0.026 x 0.005     | 0.535 x 10 <sup>-3</sup>      | 0.0065              | Not Determined       | Unstable                    |  |
| Figure 4-11(f)                       | 0.030 x 0.140         | 4.2 x 10 <sup>-3</sup>    | 2                      | 0.010 x 0.030     | 0.6 x 10 <sup>-3</sup>        | 0.010               | 25                   | Unstable                    | 0.010 Chamfer on Button                            |
| Figure 4-11(g)                       | 0.030 x 0.140         | 4.2 x 10 <sup>-3</sup>    | 2                      | 0.010 x 0.030     | 0.6 x 10 <sup>-3</sup>        | 0.010               | Not Determined       | Improved                    | See Auxiliary Supply in Figure                     |
| Figure 4-11(h)                       | 0.030 x 0.140         | 4.2 x 10 <sup>-3</sup>    | 2                      | 0.010 x 0.021     | 0.42 x 10 <sup>-3</sup>       | 0.004 See Figure    | 20                   | Unstable                    |  |
| Figure 4-11(i)                       | 0.030 x 0.140         | 4.2 x 10 <sup>-3</sup>    | 2                      | 0.010 x 0.021     | 0.42 x 10 <sup>-3</sup>       | 0.004 See Figure    | 22.5                 | Improved But Still Unstable | 2 Notches In End of Chamber                        |
| Figure 4-11(j)                       | 0.030 x 0.140         | 4.2 x 10 <sup>-3</sup>    | 2                      | 0.010 x 0.021     | 0.42 x 10 <sup>-3</sup>       | 0.004 See Figure    | 17.8                 | Improved But Still Unstable | 4 Notches In End of Chamber                        |
| Figure 4-11(k)                       | 0.030 x 0.140         | 4.2 x 10 <sup>-3</sup>    | 2                      | 0.010 x 0.022     | 0.44 x 10 <sup>-3</sup>       | 0.010 See Figure    | 20.8                 | Stable                      | Slot Length of Chamber Dia 0.080 Wide x 0.005 Deep |
| SIVA 38 Figure 4-11(l)               | 0.030 x 0.140         | 4.2 x 10 <sup>-3</sup>    | 2                      | 0.010 x 0.023     | 0.46 x 10 <sup>-3</sup>       | 0.013 See Figure    | 21.9                 | Stable                      | Slot Length of Chamber Dia 0.063 Wide x 0.005 Deep |

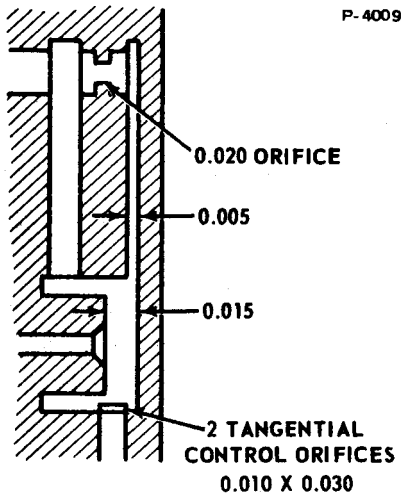
P-4009



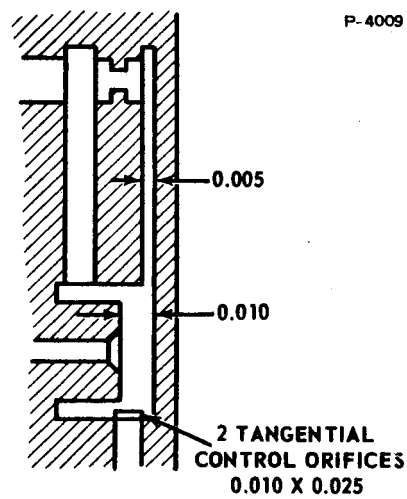
(a) Original SIVA 37 With 2 Tangential Control Orifices



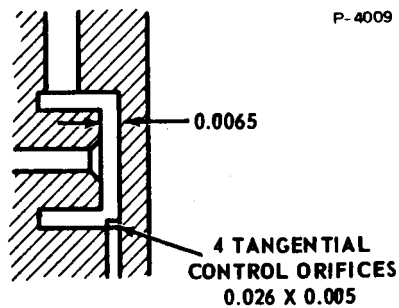
(b) Decreased Chamber Length and Rough Vortex Chamber



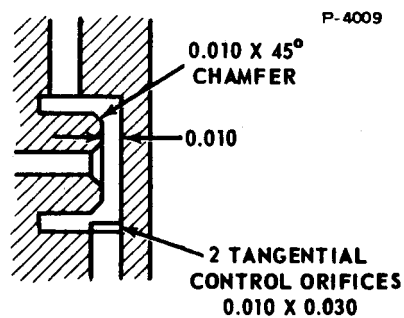
(c) Auxiliary Radial Supply



(d) Auxiliary Radial Supply With Decreased Chamber Length

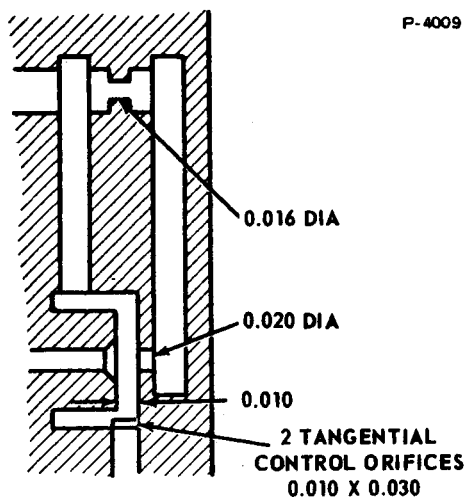


(e) 4 Tangential Control Orifices With Increased Width

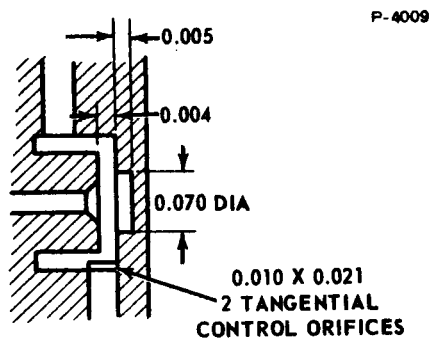


(f) Chamfered Button

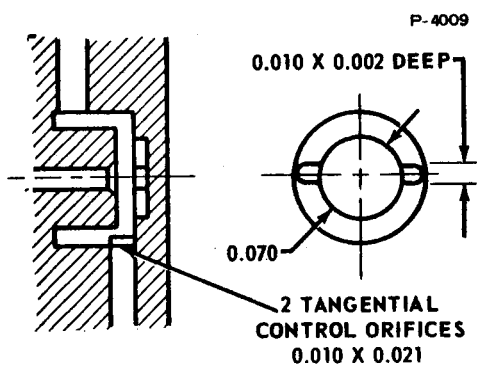
Figure 4-11 - SIVA-37 and 38 and Variations



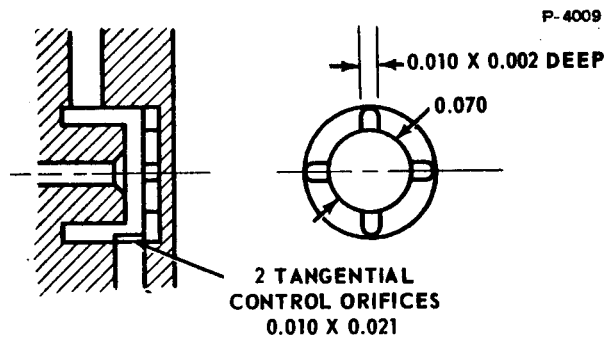
(g) Auxiliary Supply Flow In Center of Chamber



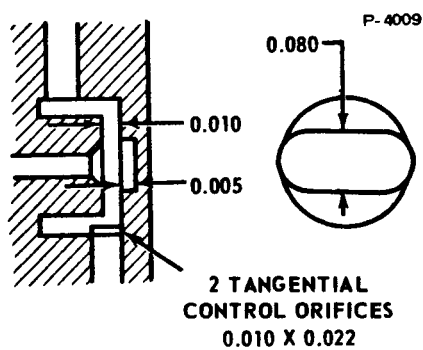
(h) Vortex Chamber With Relief In Center (Standard For Following Tests)



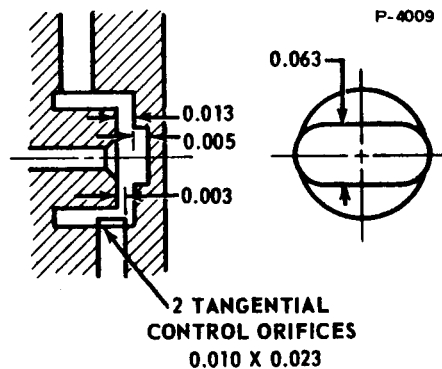
(i) Vortex Chamber With 2 Slots In End Of Chamber



(j) Vortex Chamber With 4 Slots In End Of Chamber



(k) Vortex Chamber With 0.080 Baffle In End Of Chamber



(l) SIVA 38 - 0.063 Baffle In End Of Chamber

Figure 4-11 - SIVA-37 and 38 and Variations - (Cont'd)

## SECTION 5

### GOALS OF THE FOURTH QUARTER

In the third quarter, most of the mechanical component parts have been manufactured. Virtually all of the purchased parts have been received. A breadboard lead-lag circuit was tested and demonstrated the desired lead-lag characteristics. Fluoric circuit components have been improved.

In the next quarter, the Power Control Valve, Position Error Detector Unit, and Actuator test fixture are scheduled to be completed. The final design of the fluoric circuit should be completed and tested. Actuator testing is scheduled to start during the fourth quarter.

## APPENDIX A

### VARIATION OF FREQUENCY RESPONSE WITH GAS CONSTANT AND TEMPERATURE

Consider the situation shown in Figure A-1. Gas is flowing from a supply pressure through an orifice into a volume. It is also flowing out of the volume through another orifice to an exhaust pressure. It is desired to describe pressure variations in the volume in terms of a supply pressure variation and system parameters.

In general, compressible flow can be described by the following relationship:

$$W = \frac{C_2 P_u (C_D A)_1 (P_d / P_u)}{\sqrt{T}} \quad (A-1)$$

where

$W$  = weight flow

$P_u$  = upstream pressure

$P_d$  = downstream pressure

$C_D A$  = effective area

$T$  = temperature

$C_2$  = a gas property given by

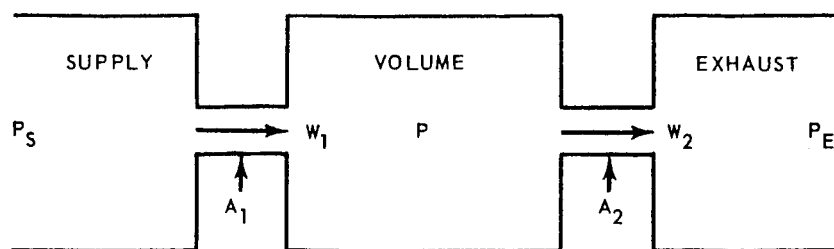
$$C_2 \equiv \sqrt{\frac{kg}{R} \left( \frac{2}{k+1} \right)^{\frac{k+1}{k-1}}}$$

where

$R$  = gas constant

$g$  = gravity constant





P-4 006

Figure A-1 - Compressible Flow Through a Tank

$k$  = specific heat ratio of the gas

$f_1(P_d/P_u)$  = function of downstream-to-upstream pressure ratio, given by

$$f_1(P_d/P_u) \equiv \sqrt{\frac{(P_d/P_u)^{2/k} - (P_d/P_u)^{\frac{k+1}{k}}}{\frac{k-1}{2} \left( \frac{2}{k+1} \right)^{\frac{k+1}{k-1}}}} \quad (A-2)$$

Equation (A-1) can be rewritten as follows

$$W = \frac{C_3 P_u (C_D A) f_1(P_d/P_u)}{\sqrt{RT}} \quad (A-3)$$

where

$$C_3 \equiv \sqrt{kg \left( \frac{2}{k+1} \right)^{\frac{k+1}{k-1}}} \quad (A-4)$$

Both  $C_3$  and  $f_1(P_d/P_u)$  are functions of specific heat ratio and pressure ratio only. Consider the case where pressure levels and flow levels are considerably higher than the amount of variation. The flow is given by

$$W_1 = W_o + \Delta W_1$$

$$W_2 = W_o + \Delta W_2$$

With orifice area and temperature constant, the weight flow variation is given by

$$\Delta W = \frac{\partial W}{\partial P_u} \Delta P_u + \frac{\partial W}{\partial P_d} \Delta P_d \quad (A-5)$$

Differentiating equation (A-3) with respect to upstream and downstream pressure,

$$\frac{\partial W}{\partial P_u} = \frac{C_3 C_D A}{\sqrt{RT}} \left[ f_1(P_d/P_u) - \frac{P_d}{P_u} f_1'(P_d/P_u) \right] \quad (A-6)$$

$$\frac{\partial W}{\partial P_d} = \frac{C_3 C_D A}{\sqrt{RT}} \left[ f_1'(P_d/P_u) \right] \quad (A-7)$$

where

$$f_1' \equiv \frac{d \left[ f_1(P_d/P_u) \right]}{d(P_d/P_u)}$$

and is a negative number (or zero as a maximum).

The equation of state is

$$M = \frac{PV}{RT}$$

Combining this with the continuity equation gives

$$\frac{dM}{dt} = \frac{d}{dt} \left( \frac{PV}{RT} \right) = \Delta W_1 - \Delta W_2 \quad (A-8)$$

Combining equations (A-5) and (A-8) gives

$$\frac{V}{RT} \frac{dP}{dt} = \frac{\partial W_1}{\partial P_s} \Delta P_s + \frac{\partial W_1}{\partial P} \Delta P - \frac{\partial W_2}{\partial \Delta P} \Delta P \quad (A-9)$$

when volume and temperature are considered to be constant. Substituting equations (A-6) and (A-7) into equation (A-9) yields

$$\begin{aligned} \frac{dP}{dt} = & \frac{C_3 \sqrt{RT}}{V} \left[ C_D A_1 \left\{ f_1 \left( \frac{P}{P_s} \right) - \frac{P}{P_s} f_1' \left( \frac{P}{P_s} \right) \right\} \Delta P_s \right. \\ & \left. + C_D A_1 \left\{ f_1' \left( \frac{P}{P_s} \right) \right\} \Delta P - C_D A_2 \left\{ f_1 (P_E/P) - \frac{P_E}{P} f_1' (P_E/P) \right\} \Delta P \right]. \end{aligned}$$

Combining terms and simplifying gives the result:

$$\begin{aligned} \left[ 1 + \frac{\frac{V}{C_3 \sqrt{RT}}}{-C_D A_1 \left\{ f_1' \left( \frac{P}{P_s} \right) \right\} + C_D A_2 \left\{ f_1 \left( \frac{P_E}{P} \right) - \frac{P_E}{P} f_1' \left( \frac{P_E}{P} \right) \right\}} S \right] \Delta P = \\ \left[ \frac{C_D A_1 \left\{ f_1 (P/P_s) - \frac{P}{P_s} f_1' (P/P_s) \right\}}{-C_D A_1 \left\{ f_1' (P/P_s) \right\} + C_D A_2 \left\{ f_1 (P_E/P) - \frac{P_E}{P} f_1' (P_E/P) \right\}} \right] \Delta P_s \quad (A-10) \end{aligned}$$

Equation (A-10) is of the form

$$(1 + \tau S) \Delta P = \frac{\partial P}{\partial P_s} \Delta P_s \quad (A-11)$$

Recalling that  $f_1'(P_d/P_u)$  is a negative number, all of the terms in equation (A-10) are positive. Comparing equations (A-10) and (A-11), the time constant  $\tau$  is seen to be directly proportional to volume, inversely proportional to  $\sqrt{RT}$ , and a complex function of pressure ratios.

The propagation velocity of a pressure wave in a perfect gas is given by

$$a = \sqrt{kgRT} \quad .$$

The time required for a pressure wave to advance a distance D is given by

$$t = \frac{D}{\sqrt{kgRT}} \quad .$$

Thus variation of time constants and transportation lags is inversely proportional to  $\sqrt{RT}$ .

Consider the change in time constants when a system is tested first with 70°F nitrogen and then with 140°F hydrogen.

$$\frac{\tau_{H_2}}{\tau_{N_2}} = \sqrt{\frac{(RT)_{N_2}}{(RT)_{H_2}}} = \sqrt{\frac{662 \times 530}{9202 \times 600}} = 0.252$$

Thus the time constants would be reduced by a factor of four when changing from 70°F nitrogen to 140°F hydrogen.

NASA-Lewis Research Center (25)  
2100 Brookpark Road  
Cleveland, Ohio 44135  
Attention: Vernon D. Gebben

NASA-Lewis Research Center (2)  
2100 Brookpark Road  
Cleveland, Ohio 44135  
Attention: Lewis Library

NASA-Lewis Research Center (1)  
2100 Brookpark Road  
Cleveland, Ohio 44135  
Attention: James E. Burnett, Technology Utilization Office

NASA-Ames Research Center (1)  
Moffett Field, California 94035  
Attention: Library

NASA-Goddard Space Flight Center (1)  
Greenbelt, Maryland 20771  
Attention: Library

NASA-Marshall Space Flight Center (2)  
Huntsville, Alabama 35812  
Attention: Library

NASA-Western Operations (1)  
150 Pico Boulevard  
Santa Monica, California 90406

NASA-Scientific & Technical Information Facility (6 & Reproducible)  
Box 5700  
Bethesda, Maryland  
Attention: NASA Representative

NASA-Lewis Research Center (1)  
2100 Brookpark Road  
Cleveland, Ohio 44135  
Attention: C. J. Shannon

NASA-Lewis Research Center (1)  
2100 Brookpark Road  
Cleveland, Ohio 44135  
Attention: Lewis Technical Information Division

NASA-Flight Research Center (1)  
P. O. Box 273  
Edwards, California 93523  
Attention: Library

NASA-Langley Research Center (1)  
Langley Station  
Hampton, Virginia 23365  
Attention: Library

NASA-Manned Spacecraft Center (1)  
Houston, Texas 77001  
Attention: Library

Jet Propulsion Laboratory (1)  
4800 Oak Grove Drive  
Pasadena, California 91103  
Attention: Library

Harry Diamond Laboratories (2)  
Washington 25, D.C.  
Attention: Library

Wright-Patterson Air Force Base (2)  
Ohio  
Attention: Library

U.S. Atomic Energy Commission (3)  
Technical Information Service Extension  
P. O. Box 62  
Oak Ridge, Tennessee

NASA-Lewis Research Center (2)  
2100 Brookpark Road  
Cleveland, Ohio 44135  
Attention: Nuclear Rocket Technology Office

NASA-Headquarters (1)  
Washington, D. C. 20546  
Attention: John E. Morrissey, NPO

Army Missile Command (2)  
Redstone Arsenal, Alabama  
Attention: Library

U. S. Atomic Energy Commission (3)  
Technical Reports Library  
Washington, D. C.